Gas-Solid Contacting with Ozone Decomposition Reaction

C. G. FRYE, W. C. LAKE, and H. C. ECKSTROM

Pan American Petroleum Corporation, Tulsa, Oklahoma

Fluidized catalyst beds have advantages in catalyst handling and heat transfer when compared with fixed beds. At a given space velocity, however, the conversion in fluidized beds is lower than that observed in fixed beds, owing to less efficient gas-solid contacting. Since the performance of fluid-bed reactors depends upon gas-catalyst contacting, their design benefits from a knowledge of the variables affecting contacting. Contacting mechanisms for fluidized beds have been proposed and tested by several investigators: Shen and Johnstone (*1*) studied the kinetics of decomposition of nitrous oxide over an impregnated alumina catalyst in fixed and fluid beds, and in a more recent paper Mathis and Watson (*2*) studied the effect of fluidization on the kinetics of catalytic cumene dealkylation in fixed and fluid beds. Both papers were concerned primarily with developing a mechanism of fluid-bed contacting by applying fluid-bed kinetic data to proposed models of fluid-bed behavior. These papers indicate that current knowledge of the contacting mechanism is insufficient to develop generalized correlations for reactor design; therefore the design of large-scale fluid-bed reactors depends upon empirical correlations developed from fluid-bed kinetic data. Unfortunately, as the number of fluid-bed parameters that may influence gas-catalyst contacting is large, experiments performed to obtain these design data with most industrial reactions are expensive and time consuming.

To reduce the expense and time required to obtain these fluid-bed kinetic data a substitute reaction may be used which has the following characteristics: low concentrations of reactant; rapid and accurate analysis by simple, well-established methods; and measurable reaction rates at low pressures and temperatures. In addition to these characteristics the substitute reaction must be rate controlled in the same way and by the same catalyst as the reaction for which it is to be substituted.

Hydrocarbon synthesis on mill-scale catalyst is a reaction for which a substitute is desirable to obtain reactor design data, and ozone decomposition was found to possess the requirements of a satisfactory substitute for this reaction.

The ozone decomposition reaction was used in 2-, 8-, and 30-in.-diam. metal reactors to obtain data for predicting fluid-bed reactor performance. In addition experiments were performed in small glass fixed- and fluid-bed reactors to investigate the mechanism of fluid-bed gas-catalyst contacting. The purpose of this paper is to discuss the results of these experiments.

C. G. Frye is at Standard Oil Company, Whiting, Indiana, and H. C. Eckstrom is at the University of Kentucky, Lexington.

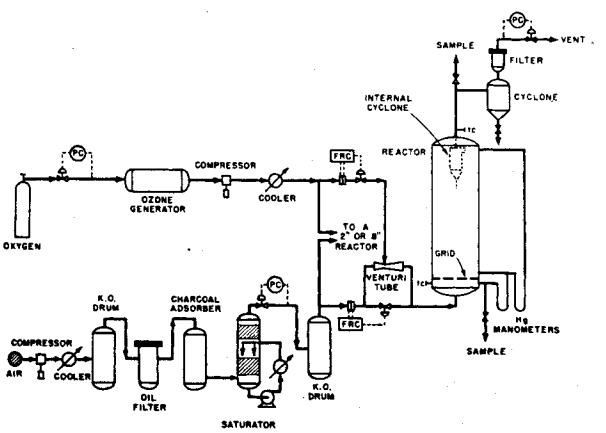

Fig. 1. Flow diagram of pilot plant experimental equipment.

EXPERIMENTAL PROCEDURE

The experimental procedures used to study fluid-bed gas-solid contacting with the ozone decomposition reaction in 2-, 8-, and 30-in.-diam. metal reactors are described under Pilot Plant Procedure. The small-diameter (11 and 22 mm.) glass-reactor experimental procedures (for both fixed and fluid beds) are described under Laboratory Procedure.

The catalyst used in these studies was rod mill scale obtained from the Bethlehem Steel Corporation plant at Sparrows Point, Maryland. The catalyst was ground to a particle size of −40 mesh, washed with boiling water twice, and air dried. Bulk settled density of the catalyst varied from 165 to 200 lb./cu. ft. and particle specific gravity from 4.5 to 5.0. Average properties for the catalysts, indicated as fine grind and coarse grind, are as follows:

Screen Analysis, Wt. %
(U. S. National Bureau of Standards)
Sieve Sizes

	Average settled catalyst density lb./cu. ft.	−40 +60	−60 +80	−80 +100	−100 +140	−140 +200	−200 +325	−325	Minimum fluidization velocity ft./sec.
Fine	165	—	—	2.6	37.8	28.4	22.0	9.2	0.05
Coarse	197	11.8	18.1	15.1	21.4	12.7	12.8	8.1	0.13

The minimum fluidization velocity was determined in separate small-scale equipment by use of nitrogen at room temperature and atmospheric pressure.

Pilot Plant Procedure

A flow diagram of the 30-in. reactor used in the pilot plant is shown in Figure 1. The 2- and 8-in. fluid units were operated with the same gas-supply system as the 30-in. unit.

Compressed air was passed through a knockout drum, felt oil filter, and charcoal adsorber to remove contaminants. Water concentration in the reactor feed was controlled by saturating the air with water at a measured pressure and temperature (usually 85 lb./sq. in. gauge and 85°F.) in a small packed tower. A portion of the air stream from the saturator was mixed with the ozone-oxygen stream in a Venturi tube, the purpose of which was to eliminate surges in the ozone-oxygen stream by absorbing the pressure changes in the main feed line to the reactor grid.

Ozone was made in a Welsbach type C ozone generator from bottled oxygen. A low nitrogen concentration was essential to avoid poisoning the catalyst with nitrogen oxides formed in the ozone generator. All valves, piping, and equipment from the ozone-generator exit to the Venturi were constructed of stainless steel.

The combined feed stream was preheated to 85°F. before entering the reactor through a multiholed flat plate grid. The reactor was insulated and electrically heated to maintain a constant temperature. Sample lines of Tygon tubing were connected to stainless steel valves just below the grid and between the reactor and external cyclone on the vent line for the 30-in.-diam. unit. For the 2- and 8-in.-diam. units sampling ports were located below the grid, on the vent line, and about 11 ft. above the grid. All three reactors were about 20 ft. long.

Air and ozone-oxygen flow rates were measured by orifice meters, static pressures by mercury manometers or pressure gauges, and temperatures by thermocouples. Most of the pilot plant experiments were conducted with atmospheric pressure at the reactor vent, although a few runs were made with about 45 lb./sq. in. gauge back pressure.

Since the comparison of the efficiencies of gas-solid contacting in different reactor systems requires a catalyst of constant activity, periodic activity checks were performed in the 8-in.-diam. unit. Before any of the reactors were loaded with catalyst, a blank run was made to measure the amount of ozone conversion due to the walls of the reactor. The ozone conversion on the walls of the 8-in. unit slowly increased with time. Instead of the reactor being replaced a new sheet-metal liner was inserted in the unit to provide a less active surface whenever the empty unit conversion became too large.

During loading of the reactors an air flow of about 0.1 ft./sec. was maintained. Ozone concentration was adjusted to 0.03 ± 0.005 mole % ozone in the total feed. After steady state conditions had been attained, two or three samples each of the reactor feed and vent gas streams were analyzed for ozone concentration by either a chemical or an optical method.

A catalyst inventory was maintained and samples taken during unloading for particle size determination. Catalyst fines were retained in the 30-in. reactor by an internal cyclone, while the fines from an external cyclone were returned at the end of each run.

The catalyst bed height (settled) was calculated from the catalyst inventory, bulk settled density, and open cross-sectional area of the reactor. Superficial gas velocity was calculated at the conditions in the top of the reactor. Experimental results were obtained at constant reactor temperature (generally 85°F. ± 0.5°) to eliminate the need for temperature corrections.

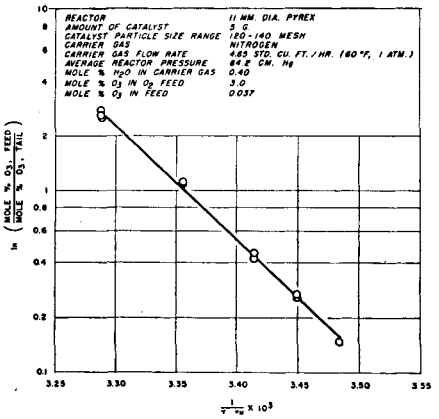

Fig. 4. Arrhenius plot for activation energy of ozone decomposition reaction.

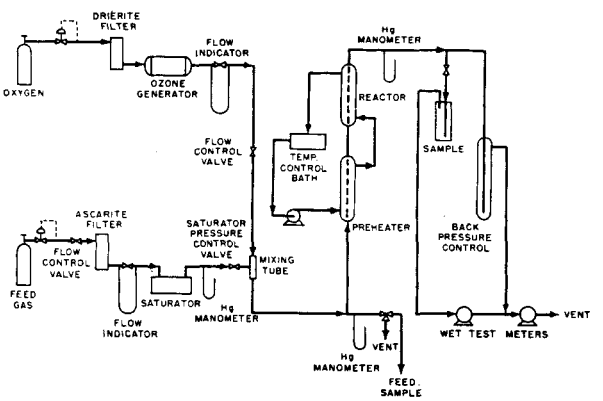

Fig. 2. Flow diagram of laboratory experimental equipment.

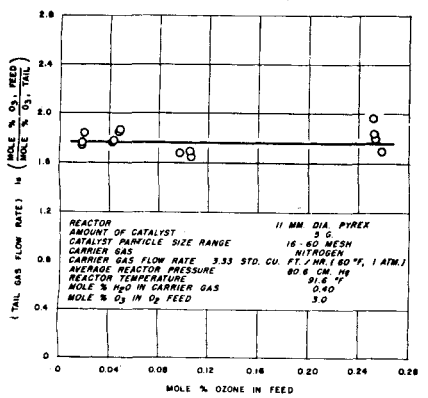

Fig. 3. Order of ozone decomposition reaction.

Laboratory Procedure

A flow diagram of the experimental equipment used with the glass reactors is shown in Figure 2. Various gases were used instead of air as the carrier gas in this system. The carrier gas stream was passed through an ascarite trap to remove small amounts of carbon dioxide and then saturated with water vapor at a controlled temperature and pressure before being throttled into the mixing tube. In a single experiment it was observed that carbon dioxide as the carrier gas poisoned the catalyst. The oxygen stream was passed through Drierite and the ozone generator before entering the mixing chamber. A constant fraction of the mixed stream was continuously withdrawn for feed gas analysis. The remainder of the mixed stream was passed through the glass preheater and through the reactor. The reactor effluent stream was analyzed chemically, and a wet test meter measured the total tail gas rate. All pressures were measured with open-end mercury manometers; temperatures were measured by mercury thermometers with 0.1°C. graduations.

An 11 mm. diam. pyrex glass reactor was used for fixed bed experiments. Downflow operation was used with the catalyst supported by a coarse fritted glass disk. A similarly constructed 22-mm. Pyrex glass reactor was used for the fluid-bed experiments. The usual catalyst charge to the 11- and 22-mm. diam. reactors was 5 and 20 g., respectively.

Analytical Procedure

Chemical Method

Ozone was determined volumetrically by the iodide method (*3*) which depends upon the reaction

$$2KI+O_3+H_2O \rightarrow I_2+O_2+2KOH.$$

Optical Method

Ozone was determined by its ultraviolet absorption using 255 mμ as the analytical wave length. A Beckman recording ultraviolet spectrophotometer with a 10-cm. absorption cell was used and calibrated with the iodide method.

RESULTS AND DISCUSSION

Fixed-Bed Kinetics of the Ozone Decomposition Reaction

A characteristic of a substitute reaction for fluidization studies is similar reaction kinetics. Consequently the kinetics of ozone decomposition over mill scale were determined in small fixed-bed glass reactors for comparison with hydrocarbon synthesis data.

Order of Reaction

To determine the order of the ozone decomposition reaction the mole fraction of ozone was varied from about 0.02 to

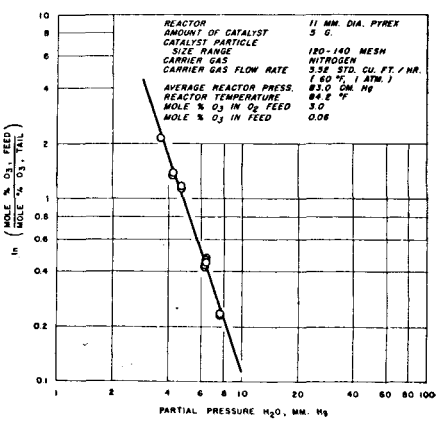

Fig. 5. Effect of water partial pressure on ozone decomposition reaction.

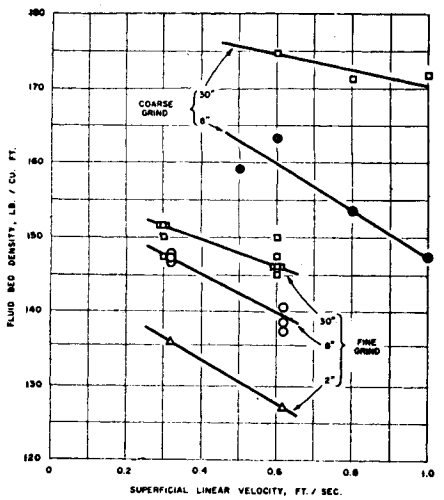

Fig. 6. Effect of linear velocity on fluid-bed density.

0.26 with all other variables held constant. The data from this experiment are shown in Figure 3. Since the product (total gas flow rate) [ln (mole % ozone, feed/mole % ozone, tail)] is constant over about a tenfold change in feed ozone concentration, it has been concluded that the reaction is first order with respect to ozone concentration. Data from similar experiments with the hydrocarbon synthesis reaction show this reaction to be first order also, as confirmed by data appearing in the literature (*4*).

Activation Energy

Activation energy of the reaction was evaluated over the temperature range from 57° to 88°F. The data are presented in Figure 4 as a plot of log [ln (mole % o_3, feed/mole % o_3, tail)] vs. $1/T$. An activation energy of about 29 kcal./g. mole was calculated from the slope of this curve. Since the magnitude of this energy of activation is consistent with a surface rate-controlled reaction, it was assumed that the ozone decomposition reaction is surface rate controlled. Data from similar experiments with the hydrocarbon synthesis reaction indicate that this reaction is also surface rate controlled (*4*).

Effect of Water Partial Pressure

To determine the effect of water upon the ozone decomposition reaction water partial pressure was varied from 3.5 to 7.5 mm. mercury holding all other variables constant, including a pressure of 1 atm. Data from this experiment are shown in Figure 5 as a plot of log [ln (mole % ozone, feed/mole % ozone, tail)] vs. log partial pressure of water in millimeters of mercury. Since the slope of the correlating line is approximately minus 3, it has been concluded that over the range investigated the reaction is reciprocal third order with respect to water vapor concentration.

Derivation and Evaluation of Reaction Rate Constants

Derivation

From the fixed-bed data discussed, rate of ozone decomposition per unit mass catalyst is equal to $k(p_{o_3}/p^3_{H_2O})$. In a differential length of reactor of cross section area, the mass of catalyst is equal to $\eta\ A\ dl$. Thus, rate of ozone decomposition in reactor segment dl is equal to $kA\eta(p_{o_3}/p^3_{H_2O})\ dl$. Under steady state conditions the moles of ozone decomposed per unit time are equal to the moles of ozone entering reactor segment dl per unit time (n_{o_3}) minus the moles of ozone leaving reactor segment dl per unit time ($n_{o_3} + dn_{o_3}$). Thus rate of ozone decomposition in reactor segment dl becomes

$$-dn_{o_3} = kA\eta \frac{p_{o_3}}{p^3_{H_2O}}\, dl$$

This may be rewritten

$$\frac{-d(N_G y_{o_3})}{y_{o_3}} = \frac{kA\eta}{y^3_{H_2O}} \frac{dl}{\pi^2} \qquad (1)$$

When the total pressure varies linearly with the length of the reactor, $\pi = a - b\eta l$. With η assumed constant, $d\pi = -b\eta\ dl$. Equation (1) may now be written

$$\frac{d(N_G y_{o_3})}{y_{o_3}} = \frac{kA}{by^3_{H_2O}} \frac{d\pi}{\pi^2} \qquad (2)$$

For the case in which the change in total moles of gas is negligible (moles total gas $\gg$ moles ozone), and temperature and mole fraction water are constant, this equation may be integrated over the length of a fixed bed and solved for k to yield

$$k = by^3_{H_2O}\left(\frac{N_G}{A}\right)\left[\frac{1}{\frac{1}{\pi_T} - \frac{1}{\pi_B}}\right] \ln \frac{(y_{o_3})_B}{(y_{o_3})_T} \qquad (3)$$

Although Equation (3) has been derived for fixed catalyst beds, it has been used in this paper as a measure of the activity of fluid catalyst beds. For fluid beds, when π is expressed in pounds per square foot and η in pounds per cubic foot, $b = 1$. Since the reaction rate constant in Equation (3) is a direct measure of fluid-bed reactor performance, this equation offers a convenient means of correlating ozone conversion data from a fluid bed. Use of Equation (3) for fluid bed data correlation purposes does not necessarily suggest any particular contacting mechanism in fluid beds.

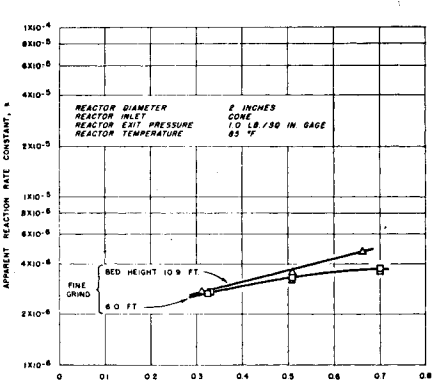

Fig. 7. Apparent reaction rate constant vs. linear velocity and bed height for 2-in. reactor.

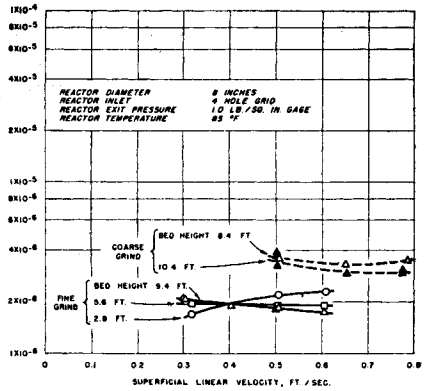

Fig. 8. Apparent reaction-rate constant vs. linear velocity, bed height, and catalyst particle size for 8-in. reactor.

Corrections for Ozone Conversion on Reactor Walls

Since the sampling point for the reactor tail gas was generally several feet above the top of the fluid bed, ozone was decomposed by the *reactor walls above the bed* before the gas was sampled and analyzed. Thus the ozone concentration at the top of the fluid bed in Equation (3) was unknown. To obtain this concentration blank runs were made without catalyst before and after each set of experiments with catalyst present. These data are sufficient to calculate the ozone concentration at the top of the fluid bed if the following assumptions are made: Rate equation (1) developed for reaction within the bed is applicable to reaction on the walls; activity of the exposed wall surface is constant; and pressure change in the empty reactor is negligible.

With these assumptions Equation (1) can be integrated from the bottom of the reactor to the top sampling point to yield the result

$$\ln \frac{(y_{o_3})_{B_1}}{(y_{o_3})_{T_2}} = \frac{k' l_{RE}}{y^3_{H_2O} \pi^2_{avg.} N_G} \qquad (4)$$

Similarly Equation (1) can be integrated from the top of the fluid bed to the top sampling point to yield

$$\ln \frac{(y_{o_3})_T}{(y_{o_3})_{T_2}} = \frac{k'(l_{RCAT} - l_{BED})}{y^3_{H_2O} \pi^2_{avg.} N_G} \qquad (5)$$

Elimination of k' from Equations (4) and (5), rearranging them, and subtracting ln $(y_{o_3})_B$ from both sides of the final equation yields the desired expression

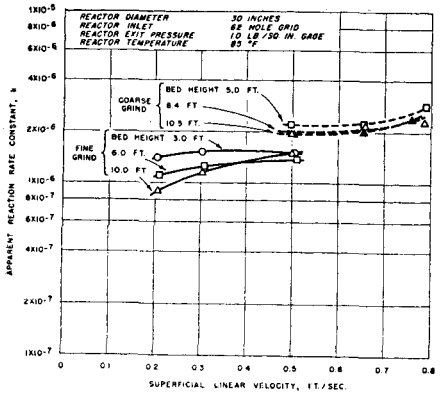

Fig. 9. Apparent reaction-rate constant vs. linear velocity, bed height, and catalyst particle size for 30-in. reactor.

to substitute in Equation (3), which then becomes

$$k = y_{H_2O}{}^3(N_G/A)\left[\ln\frac{(y_{o_3})_{T_0}}{(y_{o_3})_B} + B\,\frac{(l_{RCAT} - l_{BED})}{(l_{RE})}\ln\frac{(y_{o_3})_{B_1}}{(y_{o_3})_{T_2}}\right]\cdot\left[\frac{1}{\frac{1}{\pi_B} - \frac{1}{\pi_T}}\right] \quad (6)$$

where

$$B = \frac{[y_{H_2O}{}^3\pi_{avg.}{}^2(N_G/A)]_E}{[y_{H_2O}{}^3\pi_{avg.}{}^2(N_G/A)]_{CAT}} \quad (7)$$

and the subscripts E and CAT indicate that these quantities be evaluated at conditions used in the runs without catalyst and with catalyst, respectively. All ozone mole fractions on the right side of Equation (6) were measured.

Corrections for the ozone conversion above the bed were not greater than 10% of the apparent reaction rate constant.

Since ozone was found to be decomposed on contact with the reactor walls above the top of the fluid bed, some decomposition is also possible on the *reactor wall below the top of the fluid bed.* No correction for this conversion has been made, since the data are insufficient to calculate its extent. However it is likely to be insignificant compared to the total ozone conversion because the average actual velocity of gas within the bed is high compared to the velocity above the fluid bed, and the concentration of ozone in the dense phase of the fluid bed and therefore in contact with the reactor wall is low.

Under constant experimental conditions the precision of the data was determined, and the calculated reaction rate constant k found to deviate by a maximum of about 5%. Other experiments were performed to determine the validity of the corrections for ozone conversion on the reactor wall above the fluidized-catalyst bed. In these experiments reaction rate constants were evaluated from analyses of tail gas samples taken rapidly from the top of the reactor and from a special sample port near the top of the fluid bed. The percentage of deviation in these k values was significantly smaller than the 5% error in precision already noted.

Evaluation

Height of the fluid bed was calculated by dividing the catalyst inventory, pounds, by the cross-sectional area, square feet, and by a constant settled catalyst density, 165 lb./cu. ft., and multiplying by a constant expansion factor for fluid beds of 1.20. Pressure at the top of the bed was assumed equal to the measured pressure at the reactor exit. Pressure at the bottom of the bed was calculated by adding the bed pressure drop (measured by a mercury manometer) to the pressure at the top of the bed.

In the expression $(y_{H2O}{}^3\pi_{avg}{}^2N_G/A)_{CAT}$, the term π_{avg} lb./sq. ft. abs. was assumed to be the measured pressure at the top sampling point. In Equation (6) the following expression was evaluated from an average of data taken in the empty reactor before and after each set of experiments with catalyst present

$$\left[\ln\frac{(y_{o_3})_{B_1}}{(y_{o_3})_{T_2}}\right]\left[\frac{[y_{H_2O}{}^3\pi_{avg}{}^2(N_G/A)]_E}{l_{RE}}\right]$$

The term π_{avg} lb./sq. ft. abs. was assumed equal to the measured pressure at the top sampling point.

It should be noted that the corrections for conversion above the catalyst bed were made by using estimated fluid-bed heights. For convenience the same settled-bed density and fluid-bed expansion factor were used in all calculations. In general the corrections to the k values for ozone conversions above the catalyst bed were less than 5% of the k value. Use of actual fluid-bed heights would not significantly affect this correction for conversion above the fluid bed. Figure 6 is a plot of fluid-bed density vs. superficial linear velocity for the three reactors with coarse and fine catalysts. These data can be used to calculate actual fluid-bed heights from the settled-bed heights shown in Figures 7 to 11.

For the small-scale laboratory experiments the total pressure π in Equation (1) was assumed to be constant and equal to π_{avg}. Integration over the length of the catalyst bed gives

$$N_G \ln\frac{(y_{o_3})_F}{(y_{o_3})_T} = \frac{k}{y_{H_2O}{}^3\pi_{avg.}{}^2}(A\eta l_{BED}) \quad (8)$$

Since $W_{CAT} = A\eta l_{BED}$, the weight of catalyst in the reactor, this equation may be rearranged to read

$$k = \left[\frac{y_{H_2O}{}^3\pi_{avg.}{}^2N_G}{W_{CAT}}\right]\left[\ln\frac{(y_{o_3})_F}{(y_{o_3})_T}\right] \quad (9)$$

The apparent reaction-rate constants for both pilot plant and laboratory experiments were evaluated by using pound, foot, and second units.

Contacting Efficiency in Pilot Plant Fluid-Bed Reactors

The apparent ozone decomposition reaction-rate constant, k, evaluated from Equation (6), is a function of catalyst activity, gas-solid contacting, and temperature. When catalyst activity and temperature are held constant, k becomes a direct measure of gas-solid contacting in fluidized beds.

In Figures 7, 8, 9, and 11 the log of the rate constant k is plotted vs. linear velocity with parameters of bed height, catalyst particle size, and reactor diameter. In Figure 10 the log of the rate constant is plotted vs. the log of the reactor diameter with bed height as a parameter. Superficial linear velocities were calculated at the top of each reactor, and the bed heights (settled) were calculated from the catalyst inventory, reactor cross-sectional area, and average settled catalyst density for each grind.

Saturation temperature and pressure (which determined water concentration in the feed gas) were held constant at 85°F. and 85 lb./sq. in. gauge for the experiments shown in Figures 7 to 10; saturator temperature was increased to 90°F. for the experiments of Figure 11. All other experimental conditions are stated on the figures.

Figures 7, 8, and 9 show the effect on k of linear velocity, bed height, and particle size for reactor diameters of 2, 8, and 30 in. No coarse-grind data were available for the 2-in. reactor.

According to these three figures k appears to increase slightly as the linear velocity is increased, except for bed heights above 5.6 ft. in the 8-in. unit. Over most of the range of linear velocities studied k is shown to decrease with increased bed heights, with the exception of the 2-in. data. The most pronounced effect on k, shown by Figures 8 and 9, is due to increased particle size of the catalyst. At 0.5 ft./sec. linear velocity k increased 75% in the 8-in. unit and 40% in the 30-in. unit when the particle size

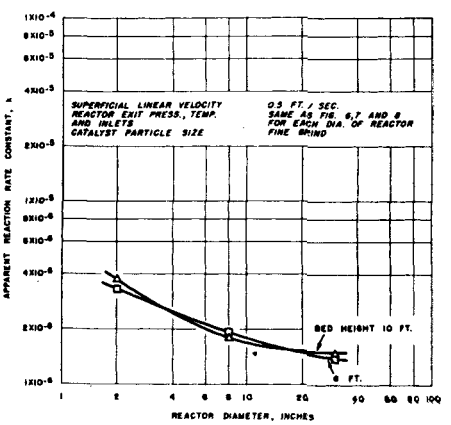

Fig. 10. Apparent reaction-rate constant vs. reactor diameter and bed height.

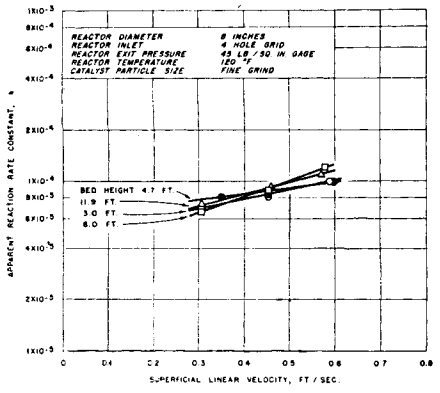

Fig. 11. Apparent reaction-rate constant vs. linear velocity and bed height for 8-in. reactor at 45 lb./sq. in. pressure.

was changed from fine to coarse grind.

Figure 10 shows the effect of reactor diameter on k with all other parameters held constant. At a bed height of 10.0 ft. and a linear velocity of 0.5 ft./sec. the ratio of k values for a 2-in. to an 8-in. reactor is 2.1 for a fine grind. This ratio, obtained with ozone decomposition, can be compared to a value of 2.3 for the ratio of 2- to 8-in. reactor performance from the hydrocarbon synthesis reaction over an iron catalyst in fluidized beds. Another comparison of the ozone decomposition with hydrocarbon synthesis can be made by using the ratios for fixed bed to 8-in. reactor performance. For these reactors the ratios are about 15 to 1 to 20 to 1 for ozone or hydrocarbon synthesis, depending on the experimental conditions. These data suggest that the ozone decomposition reaction can be used to simulate the gas-solid contacting process occurring in a hydrocarbon synthesis fluid-bed reactor. In addition these data also suggest that the ozone decomposition reaction may be used for studying gas-solid contacting in fluid beds for other first order reactions.

Figure 11 illustrates how increased reactor pressure (4 atm.) in an 8-in. reactor affects the shape of the linear-velocity–bed-height curves (Figure 8) obtained at 1-atm. pressure. At the higher pressure the effect of linear velocity appears about the same, with the bed-height effect slightly reduced. An absolute comparison between Figures 8 and 11 is complicated, since the reactor temperature was increased from 85° to 120°F. to obtain measurable ozone conversions at the higher pressure.

Preliminary Investigation of Fluid Bed Contacting Mechanism

In the preceding paragraphs no consideration has been given to the mechanism of the actual contacting process. The purpose of the experimental work discussed was to use the ozone decomposition reaction for determining the effects on gas-solid contacting of changes in certain operation variables in fluidized-bed reactors. These data suggest that ozone decomposition data may be used to develop empirical correlations for fluid-bed hydrocarbon-synthesis reactor design. However to develop generalized correlations for reactor design an understanding of the actual mechanism of gas-solid contacting is necessary.

Experiments have been performed in small glass fixed- and fluid-bed reactors by using the ozone decomposition reaction to investigate the actual contact mechanism. Such an investigation requires examination of the variables affecting gas-catalyst contacting over much wider ranges than is required for empirical reactor design. In addition parameters, which were held constant in reactor design studies, for example, catalyst activity, were varied in these preliminary mechanism studies.

This investigation began with experiments designed to determine whether the contacting process taking place in the small glass reactors is the same as that in the larger, for example, 8-in. diameter reactors. The data obtained from this preliminary study show no contradiction of an assumption that the contacting processes are the same. Two tests were made that indicated that the contacting processes were similar.

One such test was the variation of apparent reaction rate constant with temperature. In Figure 12 the quantity ln (mole % o_3, feed/mole % o_3, tail) is plotted against reciprocal temperature for a typical 22-mm.–glass-reactor experiment and for a variable-temperature run made in the 8-in.–diameter fluid reactor. The glass reactor was operated at slightly above atmospheric pressure at a gas linear velocity of about 0.44 ft./sec. and contained 20 g. of catalyst. The 8-in. reactor contained 312 lb. of catalyst and was operated at an exit pressure of 45 lb./sq. in. gauge and a linear velocity of about 0.20 ft./sec. No correction was made for empty unit conversion in the 8-in.–diameter unit. Although the conditions of operation were somewhat different (1 and 4 atm.), it is evident that the change in conversion with temperature is qualitatively similar in the two systems; thus the data suggest that the contacting process is similar in the two systems.

The other test was to investigate the effect of gas linear velocity upon gas-solid contacting. Experiments were performed in the 22-mm.–diameter reactor with nitrogen at variable flow rates as the fluidizing gas. Data from these runs are presented in Figure 13 together with similar data from a fixed-bed run with the same 120- to 140-mesh mill-scale catalyst. Each separate fluid-bed run was made with the same 20 g. of catalyst by adjusting linear velocity to a constant value and observing the change in ozone conversion with changes in temperature. Thus fluidization conditions for each run were constant. Changes in conversion were thus obtained as a function of temperature only. (Changes in linear velocity, gas density, and viscosity were small over the 30°F. temperature range used.)

Examination of Figure 13 indicates that all the fluid-bed data are correlated by a single line, although the four sets of fluid-bed data were obtained at different linear velocities. These data indicate that the effect of linear velocity is directly correlated for this particular catalyst particle size and reactor system by the first order reaction rate constant values. The data obtained with coarse catalyst in the larger diameter fluid reactor (Figures 8 and 9) also show little or no variation in k value with linear velocity, suggesting again that the contacting process in the small glass reactors is similar to that in the larger units. The corresponding data from the 2-, 8-, and 30-in.–diameter reactors, Figures 7, 8 and 9, with fine-grind catalyst (for which there are no comparable glass-reactor data) show an increase in apparent activity with linear velocity. These data suggest that the gas-catalyst contacting process may not be the same with the smaller particle-size catalyst.

Comparison of the fluid-bed with the corresponding fixed-bed activity values in Figure 13 indicates that at low conversions (about 20%) the fixed-bed activity is about 2.2 times the value for the fluid bed at the same temperature ($1/T \times 10^3 = 3.48$). The difference between the two sets of values increases with increased conversion, and so at high conversion (about 80 to 90%) the fixed-bed activity is about 5.5 times the value for the fluid bed ($1/T \times 10^3 = 3.29$). With the larger 8-in.–diameter reactor the fixed-bed value at high conversion is about fifteen to twenty times that of the fluid bed. Thus these data are consistent with the trend toward lower activity of the 8-in.–diameter reactor, compared with that of the 2-in.–diameter reactor (Figures 7 and 8).

To determine the effect of gas density upon gas-solid contacting experiments

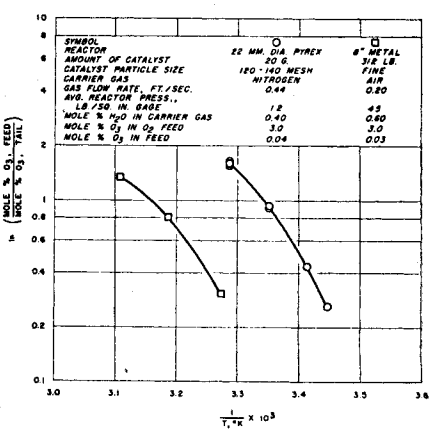

Fig. 12. Comparison of temperature effect on conversion between pilot plant and laboratory fluid-bed reactors.

were performed with helium used as the fluidizing gas. The experiments were performed in the same manner as those with nitrogen, with the same catalyst and covering the same linear velocity range. The results from these runs, which are shown in Figure 14, are not significantly different from the corresponding data with nitrogen used as the carrier gas. Since the viscosity of nitrogen and that of helium are approximately the same and the densities differ by a factor of seven, gas density is not an important factor in the gas-solid contacting process with this particular system.

The over-all kinetics of the fluidization process were determined in 11- and 22-mm.-diameter reactors. With all other variables held constant, feed-gas ozone concentration was approximately doubled. Ozone conversion in both experiments initially was 70%, and no change in percentage of conversion was observed after the feed-gas concentration had been increased. Thus it appears that under constant fluidization conditions the total conversion process is first order with respect to ozone concentration.

To determine the effect of catalyst particle size upon gas-solid contacting, experiments were performed with 60- to 100-mesh catalyst. These experiments were performed with nitrogen used as the fluidizing gas in the same manner as were the series of experiments with 120- to 140-mesh mill-scale catalyst. The data from these runs are shown in Figure 15. As in the case of the 120- to 140-mesh catalyst a single correlating line has been drawn through all the different sets of data at constant linear velocities. Close examination of Figure 15 indicates a trend toward increased k values at higher linear velocities. As in the case with the pilot plant experiments, however, this change is small.

Comparison of the fluid-bed with the corresponding fixed-bed data with the 60- to 100-mesh catalyst (Figure 15) shows that the differences are much smaller than those observed with the 120- to 140-mesh catalyst (Figure 13). At low conversions (about 20%) with 60- to 100-mesh catalyst the fixed-bed activity is about 1.4 times the values for the fluid bed at the same temperature ($1/T \times 10^3 = 3.40$). The corresponding comparison with 120 to 140-mesh catalyst was 2.2 times. At high conversions (about 80%) the fixed-bed activity is about 2.4 times the value for the fluid bed with 60 to 100 mesh catalyst ($1/T \times 10^3 = 3.25$) compared to 5.5 times with 120- to 140-mesh catalyst. Since for a fixed-temperature and catalyst-particle-size comparison of data from fixed with those from fluid beds constitutes a comparison of the effectiveness of catalyst utilization or gas-catalyst contacting, the data in Figures 13 and 15 may be interpreted to mean that the gas-solid contacting in the fluid bed with the 60- to 100-mesh catalyst is better than with the 120 to 140-mesh catalyst. In addition, since the minimum fluidization velocities for the 120- to 140-mesh catalyst and for the 60- to 100-mesh catalyst are 0.10 and 0.22 ft./sec., respectively, the improvement in gas-solid contacting may be attributed to the larger fraction of gas flowing through the dense phase of the coarser grind catalyst. Since gas flow through the voids in the dense phase is probably in the viscous range, gas viscosity should also be a variable in the gas-solid contacting mechanism.

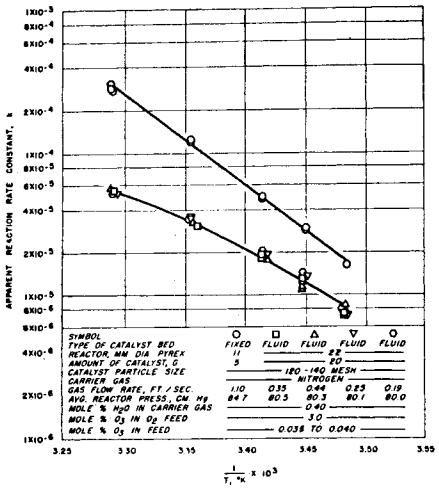

Fig. 13. Comparison of temperature effect on apparent reaction-rate constant between laboratory fixed- and fluid-bed reactors.

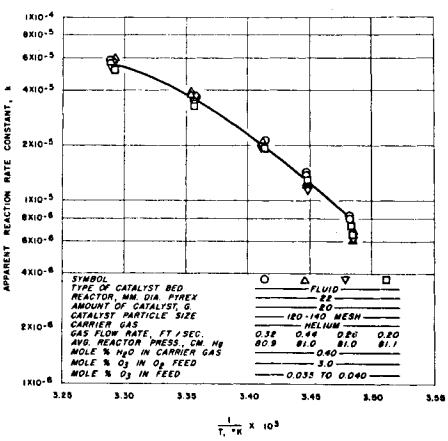

Fig. 14. Temperature effect on apparent reaction-rate constant in laboratory fluid-bed reactors.

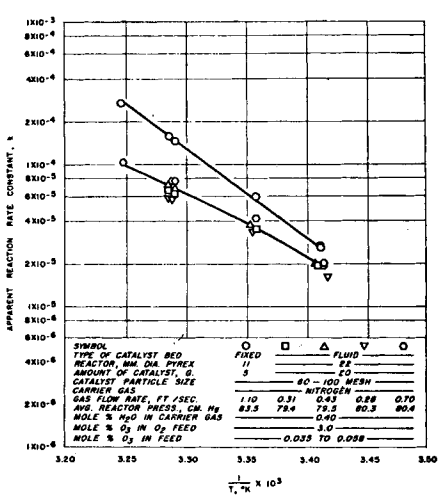

Fig. 15. Comparison of temperature effect on apparent reaction-rate constant between laboratory fixed- and fluid-bed reactors.

NOTATION

A = cross-section area of reactor
$b\eta$ = constant characteristic of catalyst bed
k = reaction rate constant per unit mass catalyst
k' = reaction rate constant per unit length
N_G = total gas flow per unit time
p_{H_2O} = partial pressure H_2O
p_{o_3} = partial pressure o_3
y_{H_2O} = mole fraction H_2O
y_{o_3} = mole fraction o_3
$(y_{o_3})_B$ = mole fraction o_3 at bottom of catalyst bed
$(y_{o_3})_{B_1}$ = ozone mole fraction at inlet for empty reactor
$(y_{o_3})_F$ = mole fraction of ozone in feed
$(y_{o_3})_T$ = mole fraction o_3 at top of catalyst bed
$(y_{o_3})_{T_2}$ = ozone mole fraction at top sampling point for empty reactor
$(y_{o_3})_{T_0}$ = ozone mole fraction at top sampling point with catalyst present
l_{BED} = height of fluid bed, ft.
l_{RCAT} = height of top sampling point above inlet with catalyst present, ft.
l_{RE} = height of top sampling point above inlet for empty reactor, ft.

Greek Letters

η = catalyst density
π = $p_{o_3}/y_{o_3} = p_{H_2O}/y_{H_2O}$ = total pressure
π_T = total pressure at top of catalyst bed, lb./sq. ft. abs.
π_B = total pressure at bottom of catalyst bed, lb./sq. ft. abs.

LITERATURE CITED

1. Shen, C. Y., and H. F. Johnstone, *A.I.Ch.E. Journal*, 1, 349 (1955).
2. Mathis, J. F., and C. C. Watson, *ibid.*, 2, 518 (1956).
3. Scott, W. W., "Scott's Standard Methods of Chemical Analysis," 5th ed., Volume 2, p. 2370, D. Van Nostrand Co., New York (1939).
4. Storch, H. H., Norma Golumbic, and R. B. Anderson, "The Fischer-Tropsch and Related Syntheses," p. 535, John Wiley & Sons, New York (1951).

Presented at A.I.Ch.E. Chicago Meeting. Manuscript received December 3, 1957; revision received April 21, 1958; manuscript accepted April 21, 1958.